



Pulse high energy Fe: ZnSe laser pumped by Q-switched Er: YAG laser

FEI XU,^{1,2} QIKUN PAN,^{1,*}  YUERU ZHANG,^{1,2} RANRAN ZHANG,¹ YI CHEN,¹ DEYANG YU,¹ AND FEI CHEN¹

¹Changchun Institute of Optics, Fine Mechanics and Physics, Chinese Academy of Sciences, Changchun 130033, China

²University of Chinese Academy of Sciences, Beijing 100049, China

*panqikun2005@163.com

Abstract: We report a pulse Fe: ZnSe laser pumped by an optical chopper Q-switched Er: YAG laser. By analyzed the spatial and temporal match of the gain and chopper, the maximum energy of the optical chopper Q-switched Er: YAG laser is 31mJ with the pulse width of 165 ns. By employing this Er: YAG laser as pump laser of Fe: ZnSe crystal, the maximum output energy of Fe: ZnSe laser is 10mJ with the pulse width of 80 ns at room temperature, that is the maximum energy of Fe: ZnSe laser at this Q-switched system to the best of our knowledge. We also study the directly Q-switched Fe: ZnSe laser, and the 2.7mJ mid-infrared laser with the pulse width of 200 ns is obtained at 80 K.

© 2023 Optica Publishing Group under the terms of the [Optica Open Access Publishing Agreement](#)

1. Introduction

Mid-infrared laser has board application in multiple fields [1–4]. And there is strong demand to compact mid-infrared solid lasers in the fields of scientific research, environmental monitoring, atmospheric remote sensing, space communication, and national defense [5–12]. The development of material crystallization techniques and advancements in doping technology have significantly propelled the progress of mid-infrared Fe: ZnSe lasers [11,13]. Uniformly doped Fe: ZnSe crystals have demonstrated enhanced gain quality within the mid-infrared wavelength range. Fe: ZnSe lasers offer unique advantages making them indispensable over other mid-infrared lasers in terms of low cost, friendly environment, compact size, huge energy, and high power.

Fe:ZnSe lasers are currently considered as one of the focal points in achieving mid-infrared laser. They can achieve short pulse laser through various Q-switched techniques. Since damage characteristics of materials, passive Q-switching and acoustic Q-switching can not to output huge energy Q-switched Fe: ZnSe laser. In 2014, Evans double-end pumped Fe: ZnSe crystal, and used the semiconductor saturable absorber mirror (SESAM) as saturable absorber at low temperature [14]. They obtained the 4045 nm laser with full-width half maximum (FWHM) of 64 ns and single energy of 600nJ. In 2017, Velikanov obtained the mid-infrared short pulse train Fe: ZnSe laser, which has about 10 Fe: ZnSe pulses and pumped by the pulse train Er: YAG laser [15]. The Er: YAG laser is Q-switched by low-doped concertation Fe: ZnSe crystal as saturable absorber. Due to the pump laser consisting of multiple pulses, the Fe: ZnSe laser cannot output a single pulse. In 2020, Hiyori Uehara used acoustic Q-switching to research Fe: ZnSe laser pumped by fiber laser [16]. They successfully attained a 4μm laser with the maximum energy of 30μJ, the pulse width of 20 ns and the repetition rate of 40kHz. In terms of mechanical Q-switching, Fedorov reported a Fe: ZnSe laser pumped by a short pulse Q-switched Er: YAG laser in 2019[17]. They used a rotation prism as a mirror of Er: YAG resonant cavity. The short pulse Fe: ZnSe laser can be outputted with the maximum energy of 5mJ. The development trends of the pulse Fe: ZnSe laser is high energy.

In this study, we achieved the pulse high energy Fe: ZnSe laser pumped by an optical chopper mechanically Q-switched Er: YAG laser. We optimized the laser structure by spatial and temporal

matching gain and chopper in the cavity. At room temperature, significant improvements were achieved in the output energy and efficiency of short-pulse Fe: ZnSe lasers. The maximum single-pulse energy reached 10mJ with a pulse FWHM of 80 ns and a slope efficiency of 35% in the mid-infrared laser. Thereafter, the output characteristics of this system were researched at different temperatures, and the pulse temporal profiles of Fe: ZnSe laser were studied. In order to compare, the performance of directly Q-switching Fe: ZnSe laser using an optical chopper was examined.

2. Optical chopper Q-switched Er: YAG laser

Fe:ZnSe crystals exhibit a significant absorption cross-section in the 3 μ m wavelength range [3,18]. Currently, Er:YAG laser is widely employed as pump lasers for Fe: ZnSe laser. Many researchers have excellent work at Q-switched Er: YAG laser [19,20]. Er: YAG lasers offer a more compact size and environmentally friendly characteristics. In this work, the Fe: ZnSe laser is pumped by an Er: YAG laser with flashlamp pumping in single pulse mode. The experimental setup is shown in Fig. 1(a). The Er: YAG crystal used in this study has dimensions of 4*100 mm with doped concentration of 50% and AR coating on the end surfaces with transmission >97% at 2.94 μ m. And it is pumped by a flashlamp with maximum energy of 87J. The temporal pulse of free-running Er: YAG laser is shown in Fig. 1(b). The Er: YAG crystal maintains the temperature by employing the hydrocooling at 298K \pm 0.5 K. The resonant cavity was formed by a flat mirror and a flat output coupler with a cavity length of 200 mm. The output coupler reflectivity is 83% at 2.94 μ m, and the mirror exhibited >99.5% reflectivity of Er: YAG laser. The pulse of Er: YAG laser is compressed by mechanical Q-switching. By employing an optical chopper for mechanical Q-switching, the maximum frequency is 1kHz with duty cycle that can be adjusted in range of 0-50%.

In the initial experiment, we obtained the Q-switched Er: YAG laser which includes a sharp and a trailing at the chopper frequency of 1kHz and duty cycle of 10%. The performance of Q-switched Er: YAG pulse is affected by the thermal effects of the trailing, in the application. It is necessary to optimize the experimental setup of the Q-switched Er: YAG laser and match the resonant laser and chopper in the cavity at the spatial and temporal, in order to mitigate the trailing and extract the sharp. As shown in Fig. 1(b), the sharp can be extracted without trailing when the chopper opening time is about 5 μ s. Since the maximum frequency of the chopper is 1kHz, we reduce the duty cycle to 0.5%, which the chopper opening time is 5 μ s. At duty cycle below 2%, the output energy of the Er: YAG laser exhibits a rapid decline. Because the chopper's physical opening is smaller than the cross-section of gain laser in the cavity. The Er: YAG laser efficiency has been greatly reduced due to the decreased gain volume inside the cavity. The maximum beam diameter of the chopper is about 0.13 mm with the duty cycle of 0.5%. The divergence angle of Er: YAG laser is 4.7 mrad, and the resonant laser has the same value in the cavity due to the cavity consisting of two flat mirrors. By employing focusing lenses with the focal length of 25 mm, the beam size can be reduced to 0.1175 mm which is smaller than the maximum beam diameter of the chopper of 0.13 mm, as shown in Fig. 1(a).

In order to Q-switched, we used a signal converter to match the lamp pumping timing and optical chopper. The lamp pump triggered by the last chopper opening and matched with the next chopper opening. By optimizing the signal delay, the laser efficiency can be improved. The optimal delay(t_c) of trigger signal of lamp can be calculated by analyzing the process of Q-switched, as shown in Fig. 1 (d). The optical chopper controller outputs the chopper sync signal upon detecting the opening of the chopper. There is a delay(t_d) between the chopper opening and the chopper signal. The signal converter transforms the chopper signal into the trigger signal with the delay(t_c). And there is a delay(t_p) between the trigger signal and the Lamp pump. The storage energy time(t_s) is about 120 μ s, since the lifetime of upper level of Er: YAG laser is 120 μ s. The storage energy rapidly consumed when the chopper opens. And the

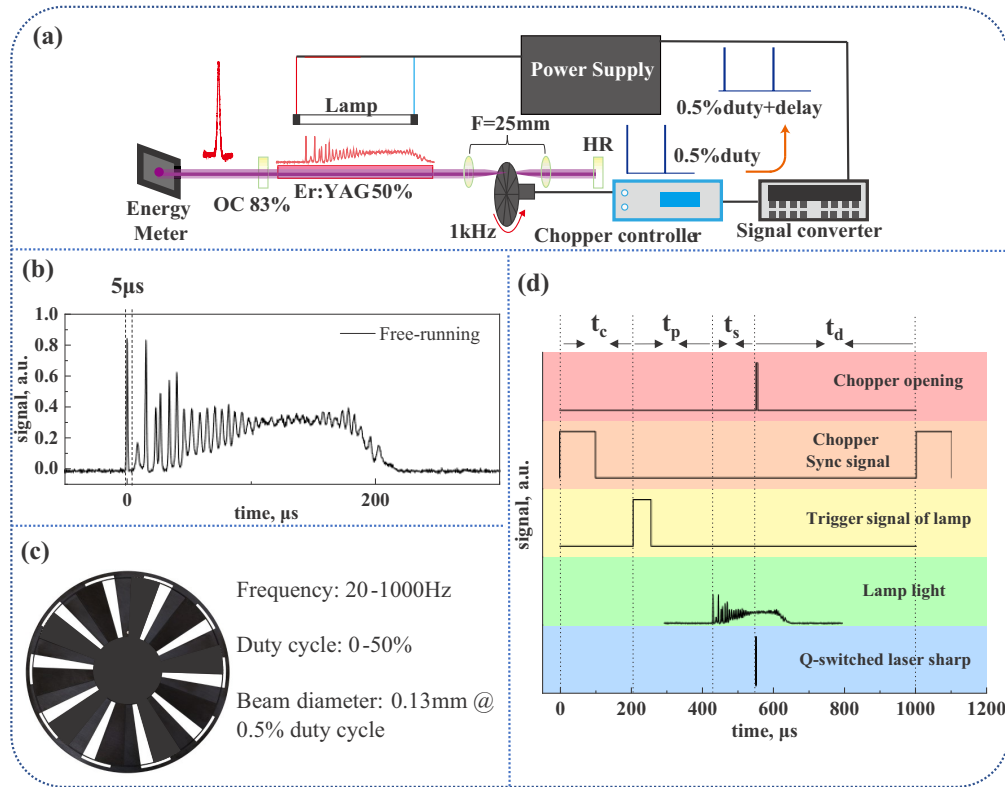


Fig. 1. (a): Experimental setup, (b): Temporal profiles of Er: YAG laser at free-running, (c): Optical chopper, (d): Process of Q-switched.

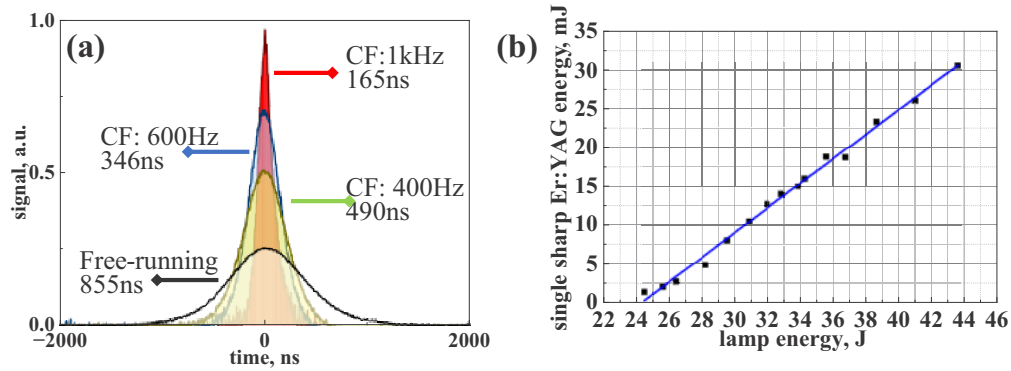


Fig. 2. Q-switched Er: YAG laser with duty cycle of 0.5%, (a): Temporal profiles of sharp at different chopper frequency (CF), (b): Dependence of output energy of Er: YAG laser on the lamp energy at chopper frequency of 1kHz, and duty of 0.5%.

Q-switched pulse of the Er: YAG laser is established. The delay t_p and t_d can be measured, and they are about $224\mu\text{s}$ and $450\mu\text{s}$ respectively. As shown in Fig. 1(d), the period of the signal is $1000\mu\text{s}$, when the frequency of the chopper is 1kHz. Therefore, the optimal delay t_c is about $206\mu\text{s}$.

There is only a sharp without the trailing at the duty cycle of 0.5%, as shown in Fig. 2(a). The peak power of the Er: YAG laser single pulse at the Q-switched is about 4 times higher than it works at free-running when the chopper frequency is 1kHz. The maximum energy of Er: YAG laser is 30mJ with the FWHM of the pulse of 165 ns. Figure 2(b) is the efficiency figure of the Er: YAG laser. The output energy of Er: YAG laser exhibits a linear response to the flash lamp energy without the saturation effect. Figure 3 is the spatial beam profiles of Er: YAG laser, which $M_x^2 = 3.17$, $M_y^2 = 3.15$.

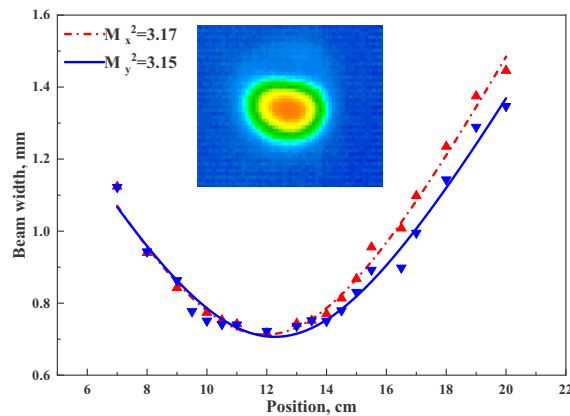


Fig. 3. The spatial beam profiles of Q-switched Er: YAG laser

3. Pulse Fe: ZnSe laser pumped by Q-switched Er: YAG laser

In order to obtain the short pulse output of Fe: ZnSe laser at room temperature, the Q-switched Er: YAG laser is used as the pump laser. And the pulse Fe: ZnSe laser characteristics are researched at different temperature.

The experimental setup of Fe: ZnSe laser is shown in Fig. 4. The Er: YAG laser with the pulse width of about 200 ns is injected the Fe: ZnSe crystal through two reflections. The pumping spot size and density can be adjusted by the 2× telescope system, and the optical spacing adjustment range is from 20 mm to 70 mm. M_1 and M_4 are mirrors of resonant cavity. M_1 is the input mirror with transmittance >98% at 2.94 μ m and reflectivity >99.5% at 4-4.6 μ m. M_4 is the output coupler with reflectivity of 75% at 4-4.6 μ m and reflectivity >99.9% at 2.94 μ m. M_2 and M_3 are window mirrors of the vacuum chamber, which can experiment at low temperatures. The Fe: ZnSe crystal is shown in Fig. 4(c). It is grown by the Bridgemen method with the size of 20×20×7mm³ and doping during growth with Fe²⁺ doped concentration of 2×10¹⁸cm⁻³. The light pass surfaces have AR coating at 3~5 μ m. The energy and temporal profiles of the laser are measured by two Pyroelectric energy meter and two HgCdTe photodetectors respectively. The temporal profile of Fe: ZnSe laser is shown in Fig. 4(a). The pulse Fe: ZnSe laser is obtained.

Fe: ZnSe laser exhibits high gain and low threshold since it is energy level structure [21]. The single pulse of Fe: ZnSe laser includes a sharp and a trailing. The delay between the Fe: ZnSe laser and pump laser decrease with the pump energy increase, at the same time the tailing gradually increases. As shown in Fig. 5, the tailing is higher than sharp and the delay between laser and pumping decreases from 200 ns to 100 ns at the pump energy increase to 31mJ. The pulse width of the Fe: ZnSe laser expands with pump energy increasing.

Fe: ZnSe laser has different performance at different temperatures [22]. The liquid nitrogen Dewar temperature controller is employed by controlling the temperature at 80K~300K ± 0.1 K. The upper-level lifetime and absorption cross section change with the change in temperature

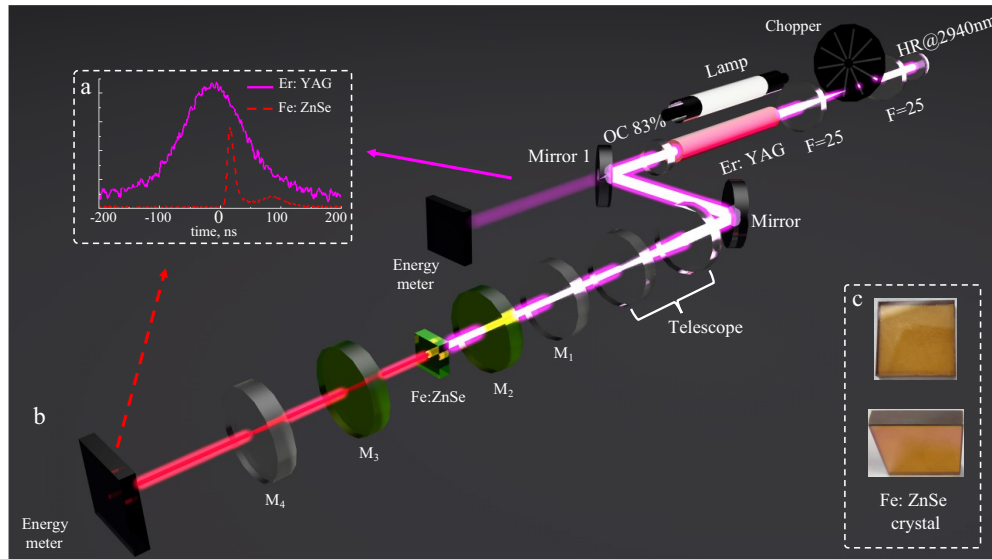


Fig. 4. Fe: ZnSe laser pumped by Q-switched Er: YAG laser, (a): Temporal profiles of pump laser and Fe: ZnSe laser. (b): Experimental setup. (d): Fe: ZnSe crystals

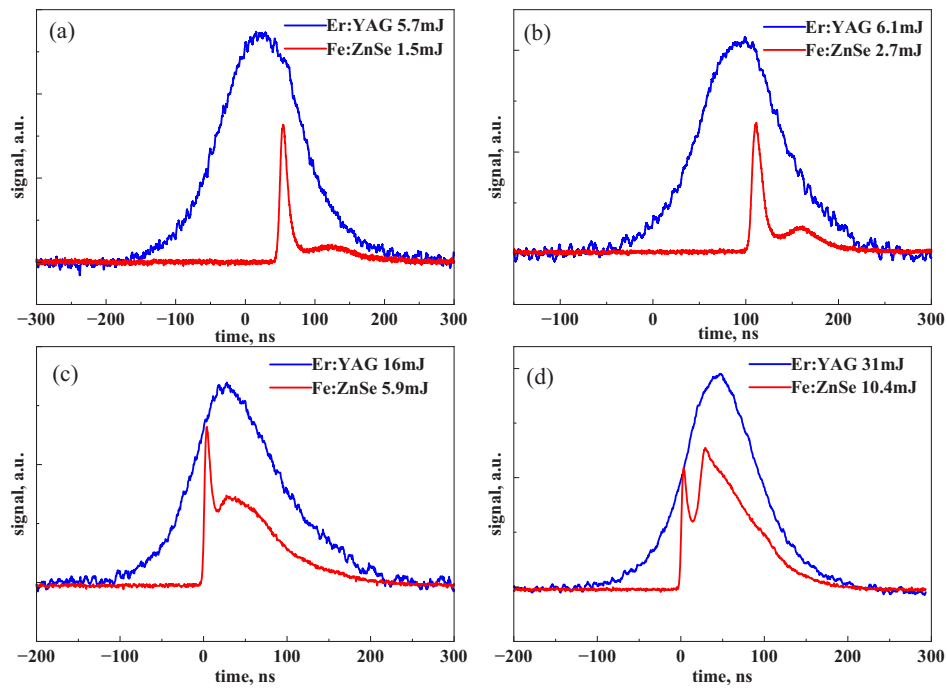


Fig. 5. Temporal profiles of Fe: ZnSe laser of different pump energy at room temperature

[3,22]. Since this, the efficiency and wavelength are influenced. As shown in Fig. 6(a), the efficiency of pulse Fe: ZnSe laser pumped by Q-switched Er: YAG laser is 35% at the RT (room temperature). And the maximum energy of Fe: ZnSe laser is 10.4mJ with a pulse width of 80 ns at RT, when it is pumped by an optical chopper Q-switched Er: YAG laser with the energy

of 31mJ and the energy density of 0.61J/cm². Since the upper-level lifetime and absorption cross section at 80 K are better than that at 295 K, the efficiency and output energy at 80 K is slightly higher than that at RT. Figure 6(b) is the output wavelength of Fe: ZnSe laser at different temperatures. The presence of multiple vibrational levels in the energy level of Fe: ZnSe laser leads to a broad emission spectrum. And the output wavelength experiences a redshift as the temperature rises. As shown in Fig. 6 (b), the center wavelength is 4091 nm with an FWHM of 40 nm at 80 K. When the temperature is set to 295 K, the center wavelength shifts to 4409 nm with an FWHM of 80 nm. Since the Fe: ZnSe crystal has high gain, the high-order modes have oscillation and output. The Fe: ZnSe laser has inferior beam quality, which is $M_x^2 = 5.12$ and $M_y^2 = 5.46$, as shown in Fig. 7. It needs optimal in the next work.

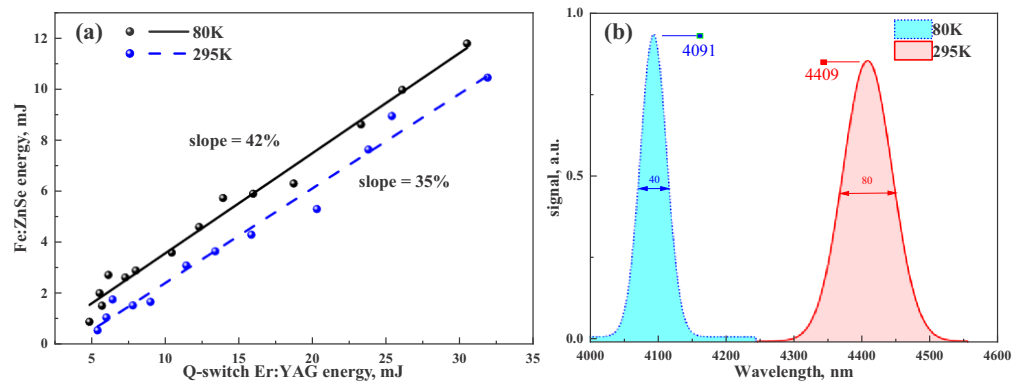


Fig. 6. The performance of Fe: ZnSe laser at different temperatures. (a): Efficiency at 80 K and 295 K. (b): Wavelength at 80 K and 295 K.

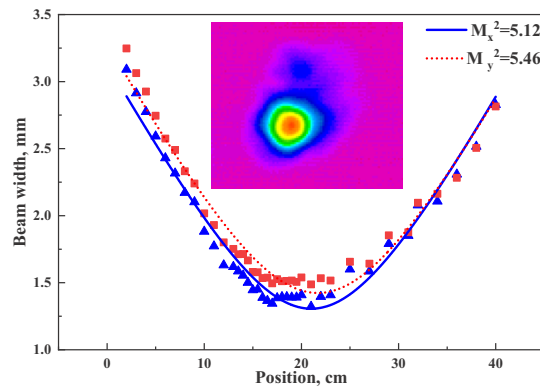


Fig. 7. The spatial beam profiles of Fe: ZnSe laser

4. Optical chopper Q-switched Fe:ZnSe laser at 80K

The optical chopper is directly employed in the resonant cavity of Fe: ZnSe laser. The Q-switched Fe: ZnSe laser is shown in Fig. 8(a). The frequency and duty cycle of the optical chopper are 1kHz and 0.5% respectively. The output energy of Q-switched Fe: ZnSe laser is just 2.7mJ with the pulse FWHM of about 200 ns at the pump energy of 700mJ with the flash lamp energy of 34J. In the same energy of flash lamp, the output energy of Fe: ZnSe laser pumped by Q-switched Er: YAG laser is 6mJ with the pulse FWHM of 80 ns. The mechanical Q-switched Fe:ZnSe laser

has inferior performance in generating pulse laser compared to the Fe:ZnSe crystal pumped by mechanical Q-switching Er:YAG laser, both in terms of efficiency and output pulse width. There are some reasons cause this result. The upper-level lifetime of Fe: ZnSe laser ($50\mu\text{s}@80\text{K}$ [23]) is shorter than that of Er: YAG laser ($120\mu\text{s}@RT$) which is not conducive to energy storage. Since the Fe: ZnSe crystal has high gain, it has stronger thermal effects and transverse parasitic oscillations [24]. The thermal effects pose a greater challenge in the matching between the gain and the chopper in the cavity. And the transverse parasitic oscillations lead to the depletion of particles in the upper energy level. Additionally, the oscillating laser between the crystal surface and the input mirror also depletes the stored energy.

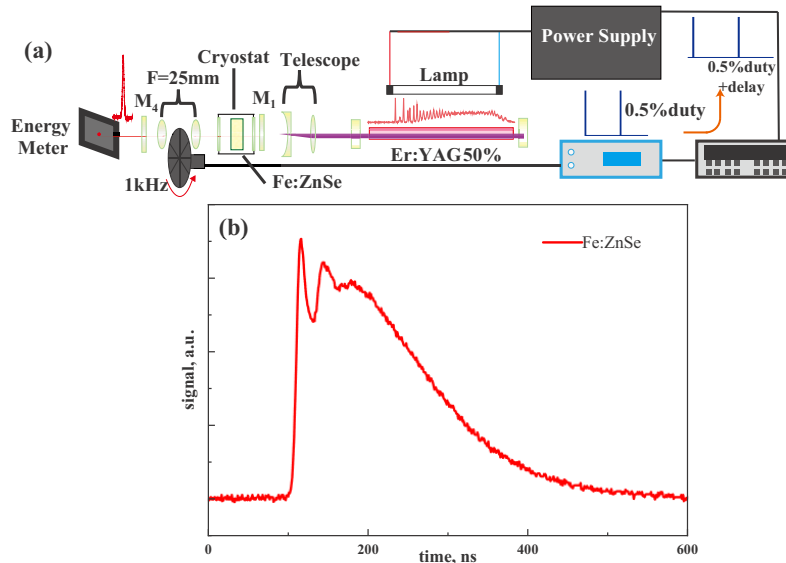


Fig. 8. Q-switched Fe: ZnSe laser. (a): Experimental setup. (b): Temporal profile of Fe: ZnSe laser

5. Conclusions

In this work, we study the pulse Fe: ZnSe laser pumped by the optical chopper Q-switched Er:YAG laser. The single pulse maximum energy of Fe: ZnSe laser is 10mJ with the pulse width of 80 ns, slope efficiency of 35%, and wavelength of $4.4\mu\text{m}$ at room temperature. The wavelength of Fe: ZnSe laser has red shift as the temperature rises. Additionally, the directly Q-switched Fe: ZnSe laser by optical chopper is studied which is pumped by a free-running Er: YAG laser. We obtained 2.7mJ mid-infrared laser with the pulse width of 200 ns at 80 K through this directly mechanical Q-switched Fe: ZnSe laser. This research results could promote the development of pulse mid-infrared solid stater Fe: ZnSe laser.

Funding. National Key Research and Development Program of China (2018YFE0203202); Natural Science Foundation of Jilin (20220101207JC); Youth Innovation Promotion Association of the Chinese Academy of Sciences (2021216).

Disclosures. The authors declare no conflicts of interest.

Data availability. Data underlying the results presented in this paper may be available from the corresponding author upon reasonable request.

References

1. N. Hoghooghi, S. Xing, P. Chang, D. Lesko, A. Lind, G. Rieker, and S. Diddams, "Broadband 1-GHz mid-infrared frequency comb," *Light: Sci. Appl.* **11**(1), 264 (2022).

2. M. Yan, P.-L. Luo, K. Iwakuni, G. Millot, T. W. Hänsch, and N. Picqué, "Mid-infrared dual-comb spectroscopy with electro-optic modulators," *Light: Sci. Appl.* **6**(10), e17076 (2017).
3. J. J. Adams, C. Bibeau, R. H. Page, D. M. Krol, L. H. Furu, and S. A. Payne, "4.0-4.5- μm lasing of Fe : ZnSe below 180 K, a new mid-infrared laser material," *Opt. Lett.* **24**(23), 1720–1722 (1999).
4. X. Zong, H. Hu, G. Ouyang, J. Wang, R. Shi, L. Zhang, Q. Zeng, C. Zhu, S. Chen, C. Cheng, B. Wang, H. Zhang, Z. Liu, W. Huang, T. Wang, L. Wang, and X. Chen, "Black phosphorus-based van der Waals heterostructures for mid-infrared light-emission applications," *Light: Sci. Appl.* **9**(1), 114 (2020).
5. L. Jumpertz, K. Schires, M. Carras, M. Sciamanna, and F. Grillot, "Chaotic light at mid-infrared wavelength," *Light: Sci. Appl.* **5**(6), e16088 (2016).
6. S. B. Mirov, I. S. Moskalev, S. Vasilyev, V. Smolski, V. V. Fedorov, D. Martyshkin, J. Peppers, M. Mirov, A. Dergachev, and V. Gapontsev, "Frontiers of Mid-IR Lasers Based on Transition Metal Doped Chalcogenides," *IEEE J. Sel. Top. Quantum Electron.* **24**(5), 1–29 (2018).
7. Y. Ma, T. Liang, S. Qiao, X. Liu, and Z. Lang, "Highly Sensitive and fast hydrogen detection based on light-induced thermoelastic spectroscopy," *Ultrafast Sci.* **3**, 0024 (2023).
8. Y. F. Ma, R. Lewicki, M. Razeghi, and F. K. Tittel, "QEPAS based ppb-level detection of CO and N₂O using a high power CW DFB-QCL," *Opt. Express* **21**(1), 1008–1019 (2013).
9. C. Zhang, S. Qiao, Y. He, S. Zhou, L. Qi, and Y. Ma, "Differential quartz-enhanced photoacoustic spectroscopy," *Appl. Phys. Lett.* **122**(24), 241103 (2023).
10. X. Xue, M. Chen, Y. Luo, T. Qin, X. Tang, and Q. Hao, "High-operating-temperature mid-infrared photodetectors via quantum dot gradient homojunction," *Light: Sci. Appl.* **12**(1), 2 (2023).
11. S. D. Velikanov, N. A. Zaretsky, E. A. Zotov, V. I. Kozlovsky, Y. V. Korostelin, O. N. Krokhin, A. A. Maneshkin, Y. P. Podmar'kov, S. A. Savinova, Y. K. Skasyrsky, M. P. Frolov, R. S. Chuvatkin, and I. M. Yutkin, "Investigation of Fe: ZnSe laser in pulsed and repetitively pulsed regimes," *Quantum Electron.* **45**(1), 1–7 (2015).
12. R. Chikkaraddy, A. Xomalis, L. A. Jakob, and J. J. Baumberg, "Mid-infrared-perturbed molecular vibrational signatures in plasmonic nanocavities," *Light: Sci. Appl.* **11**(1), 19 (2022).
13. S. B. Mirov, V. Fedorov, D. Martyshkin, I. Moskalev, and S. Vasilyev, "High Average Power Fe:ZnSe and Cr:ZnSe Mid-IR Solid State Lasers," in *Advanced Solid State Lasers* (2015).
14. J. W. Evans, P. A. Berry, and K. L. Schepler, "A Passively Q-Switched, CW-Pumped Fe:ZnSe Laser," *IEEE J. Quantum Electron.* **50**(3), 204–209 (2014).
15. S. D. Velikanov, E. M. Gavrishchuk, N. G. Zakharov, V. I. Kozlovsky, Y. V. Korostelin, V. I. Lazarenko, A. A. Maneshkin, Y. P. Podmar'kov, E. V. Saltykov, Y. K. Skasyrsky, M. P. Frolov, V. S. Tsykin, R. S. Chuvatkin, and I. M. Yutkin, "Efficient operation of a room-temperature Fe²⁺: ZnSe laser pumped by a passively Q-switched Er : YAG laser," *Quantum Electron.* **47**(9), 831–834 (2017).
16. H. Uehara, T. Tsunai, B. Y. Han, K. Goya, R. Yasuhara, F. Potemkin, J. Kawanaka, and S. Tokita, "40 kHz, 20 ns acousto-optically Q-switched 4 μm Fe:ZnSe laser pumped by a fluoride fiber laser," *Opt. Lett.* **45**(10), 2788–2791 (2020).
17. V. V. Fedorov, D. V. Martyshkin, K. Karki, and S. B. Mirov, "Q-switched and gain-switched Fe:ZnSe lasers tunable over 3.60–5.15 μm ," *Opt. Express* **27**(10), 13934–13941 (2019).
18. Q. Pan, J. Xie, F. Chen, K. Zhang, D. Yu, Y. He, and J. Sun, "Transversal parasitic oscillation suppression in high gain pulsed Fe²⁺:ZnSe laser at room temperature," *Opt. Laser Technol.* **127**, 106151 (2020).
19. K. Karki, S. Subedi, D. Martyshkin, V. Fedorov, and S. Mirov, "Recent Progress in Mechanically Q-switched 2.94 μm Er:YAG - promising pump source for 4- μm Room Temperature Fe:ZnSe Lasers," in *Conference on Solid State Lasers XXIX - Technology and Devices* 1125913 (2020).
20. K. Karki, V. Fedorov, D. Martyshkin, and S. Mirov, "High energy (0.8 J) mechanically Q-switched 2.94 μm Er:YAG laser," *Opt. Express* **29**(3), 4287–4295 (2021).
21. F. Xu, Q. K. Pan, F. Chen, Y. Chen, Y. He, K. Zhang, D. Y. Yu, J. J. Sun, and R. R. Zhang, "Theoretical characteristics of mid-infrared gain switched pulsed iron-doped ZnSe laser," *Opt. Laser Technol.* **152**, 108173 (2022).
22. J. W. Evans, T. R. Harris, B. R. Reddy, K. L. Schepler, and P. A. Berry, "Optical spectroscopy and modeling of Fe²⁺ ions in zinc selenide," *J. Lumines.* **188**, 541–550 (2017).
23. N. S. Myoung, V. V. Fedorov, S. B. Mirov, and L. E. Wenger, "Temperature and concentration quenching of mid-IR photoluminescence in iron doped ZnSe and ZnS laser crystals," *J. Lumines.* **132**(3), 600–606 (2012).
24. M. P. Frolov, Y. V. Korostelin, V. I. Kozlovsky, Y. P. Podmar'kov, and Y. K. Skasyrsky, "High-energy thermoelectrically cooled Fe: ZnSe laser tunable over 3.75-4.82 μm ," *Opt. Lett.* **43**(3), 623–626 (2018).